Ultrafast, *in-situ* Transformation of Protective Layer on Lithium-Rich Manganese-Based Layered Oxides for High-performance Li-ion Batteries

Yun-Chao Yin[1,2,3], Yan Li[1], Xueshan Hu[3], Zhi Zou[3], Yuanmao Chen[5], Zheng Liang[5], Lihui Zhou[4]*, Jinlong Yang[1]*, Jiayu Wan[3]*

[1] Guangdong Provincial Key Laboratory of New Energy Materials Service Safety, Guangdong Research Center for Interfacial Engineering of Functional Materials, College of Materials Science and Engineering, Shenzhen University, Shenzhen 518060, China

[2] College of Physics and Optoelectronic Engineering, Shenzhen University, Shenzhen 518060, China

[3] Future Battery Research Center, Global Institute of Future Technology, Shanghai Jiaotong University, Shanghai 200240, China

[4] Key Laboratory for Advanced Materials and Feringa Nobel Prize Scientist Joint Research Center, School of Chemistry & Molecular Engineering, East China University of Science and Technology, Shanghai 200237, P.R. China

[5] Frontiers Science Center for Transformative Molecules, School of Chemistry and Chemical Engineering, Shanghai Jiao Tong University, Shanghai 200240, P. R. China

Experimental Section

Synthesis of LMLO

The sample was synthesized via a co-precipitation process. Specifically, nickel, cobalt, and manganese sulfates were dissolved into a salt solution at a molar ratio of 1.6:1.7:6.7. Dilute ammonia and sodium hydroxide solutions were prepared for subsequent use. An automatic reaction kettle served as the reaction vessel, with ammonia water and sodium hydroxide solution pumped in as the bottom liquid, regulating the bottom liquid pH to 12.30 and the ammonia concentration to 12-12.5 g/L. Simultaneously, nitrogen gas was introduced to maintain a low oxygen content within the kettle. Subsequently, ammonia, alkali, and salt were simultaneously introduced. Throughout the reaction, stability of indicators such as ammonia concentration and pH were maintained, leading to a gradual increase in particle size to the desired value. Upon reaching the required output, the reaction was terminated, yielding a slurry. The slurry underwent multiple washes with water and dilute alkali before being dried in an oven. Following natural cooling, a black precursor was obtained for subsequent use. This precursor was then blended with lithium carbonate and subjected to calcination, which involved three successive steps: pretreatment at 500°C for 6 hours, followed by calcination at 710°C for 2 hours, and finally at 910°C for 12 hours. The resulting material was collected in a sample bag for future use, with the entire calcination process conducted under an oxygen atmosphere.

Synthesis of LMLO-Ov

At the outset, the LMLO powder underwent compression into pellets. Following this, the sample was positioned between two sheets of carbon paper within an argon-filled glovebox and subjected to 8 seconds of Joule heating. This heating was induced by passing current through the carbon paper to create materials rich in surface oxygen vacancies. Monitoring of temperature during the reaction was conducted using an infrared camera. Lastly, the sample was ground into powder, preparing it for subsequent battery assembly.

Electrode preparation and electrochemical methods

The cathode slurry was formulated by blending cathode materials, PVDF, and acetylene black at an 8:1:1 mass ratio dissolved in NMP. Following this, the slurry was applied onto the Al foil and subsequently vacuum-dried. The cathode electrode exhibited a mass loading ranging from 3 to 4 mg/cm^{-2}. Assembling half-cells entailed using the prepared samples as the cathode, Li foil as the counter electrode, a polyethylene porous membrane (16 μm, SK IE Technology Co., Ltd.) as the separator, and a 1.0 mol/L $LiPF_6$ solution in EC/DMC/EMC (1:1:1) containing 2% LiDFOB as additive as the electrolyte. Galvanostatic charge/discharge cycles and rate performance tests were conducted at 1C following one cycle from 2 to 4.8 V and four cycles from 2 to 4.7 V at a current density of 0.1C (1C=200 mAh/g). Electrochemical impedance spectroscopy (EIS) measurements were executed at an amplitude of 5 mV and a frequency range

spanning from 100 kHz to 0.1 Hz. For the Galvanostatic Intermittent Titration Technique (GITT), the coin cells underwent 1 cycle of charge-discharge to achieve activation and surface oxygen release before being subjected to loops of 10 minutes charge or discharge at a current of 0.1C, followed by a 2-hour relaxation period until the voltage reached upper or lower limitations.

Materials Characterization

The structural analysis utilized XRD (Rigaku, Cu Kα radiation, λ = 1.5406 Å) at a scanning rate of 5° min^{-1}, spanning the 2θ range of 5 to 90°. Material composition and element valence states were assessed via XPS (PHI 5000 VersaProbe III). Microstructural examination was conducted using an SEM (Sigma 300). Aberration-corrected STEM characterization was performed using a ThermoFisher Themis Z microscope operating at 300 kV equipped with two aberration correctors. HAADF-STEM images were captured with convergence semi-angle, inner- and outer collection angles set at 25 mrad, 47 mrad, and 200 mrad, respectively. Energy dispersive X-ray spectroscopy (EDS) utilized 4 in-column Super-X detectors. The corresponding analysis of Fast Fourier Transform (FFT) was conducted using Digital Micrograph (DM). The DEMS cells were assembled utilizing a coin cell mold within an argon-filled glovebox. Prior to conducting the DEMS tests, the assembled cells were allowed to stand for 6 hours, followed by flushing with pure argon for 3 hours to eliminate any residual air. The evolved gases were subsequently analyzed using a quadrupole mass spectrometer (QAS 100, Shanghai Linglu).

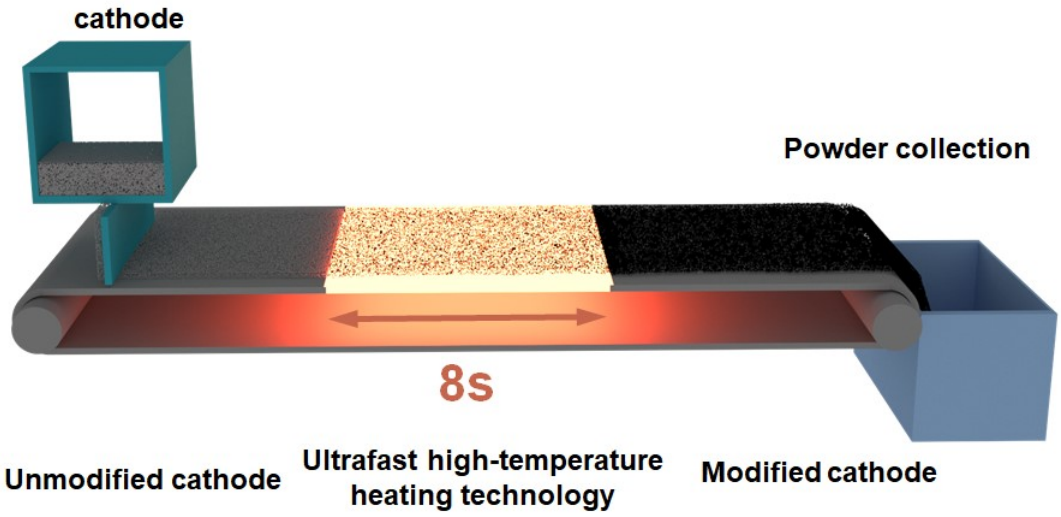

Figure S1. Schematic of the roll-to-roll production process for the surface modification of cathode materials employing ultrafast high-temperature heating technology.

we propose an ultrafast roll-to-roll manufacturing process for the surface modification of cathode materials. In this process, cathode materials continuously traverse a heating zone, facilitating the *in situ* formation of a protective layer on the material surface following rapid high-temperature treatment. This approach leverages ultrafast high-temperature heating technology, rendering the rapid modification of cathode materials highly compatible with existing industrial production protocols. This design holds significant promise for the ultrafast and efficient roll-to-roll modification of cathode materials.

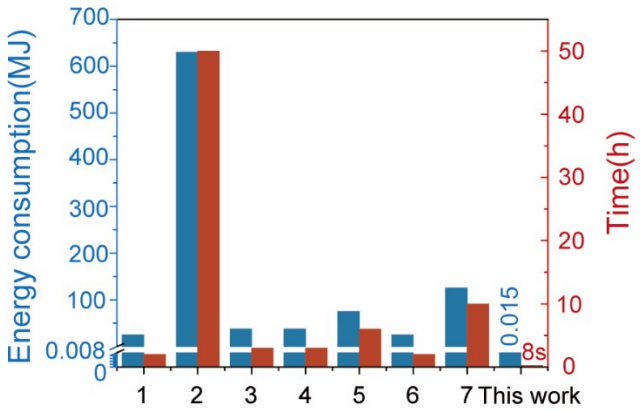

Figure S2. Comparison of Time and Energy Consumption in Different Methods for Introducing Spinel and Oxygen Vacancies on the Surface of Lithium-Rich Manganese Cathode Materials

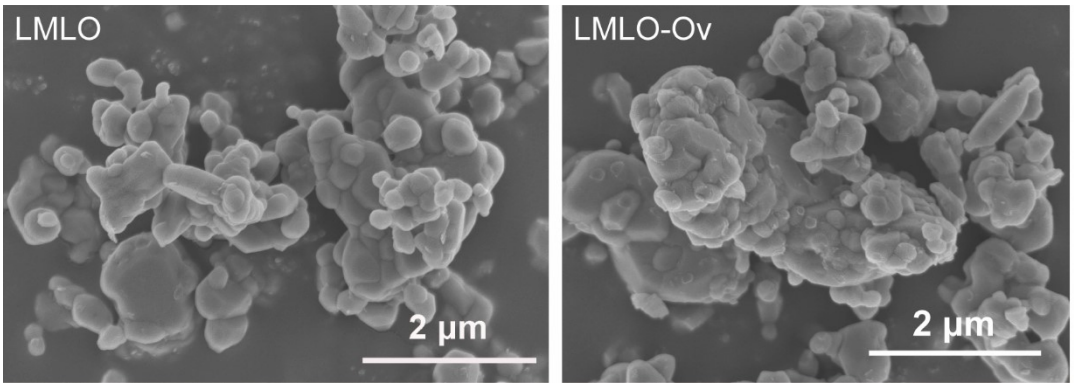

Figure S3. SEM image of the LMLO and LMLO-Ov.

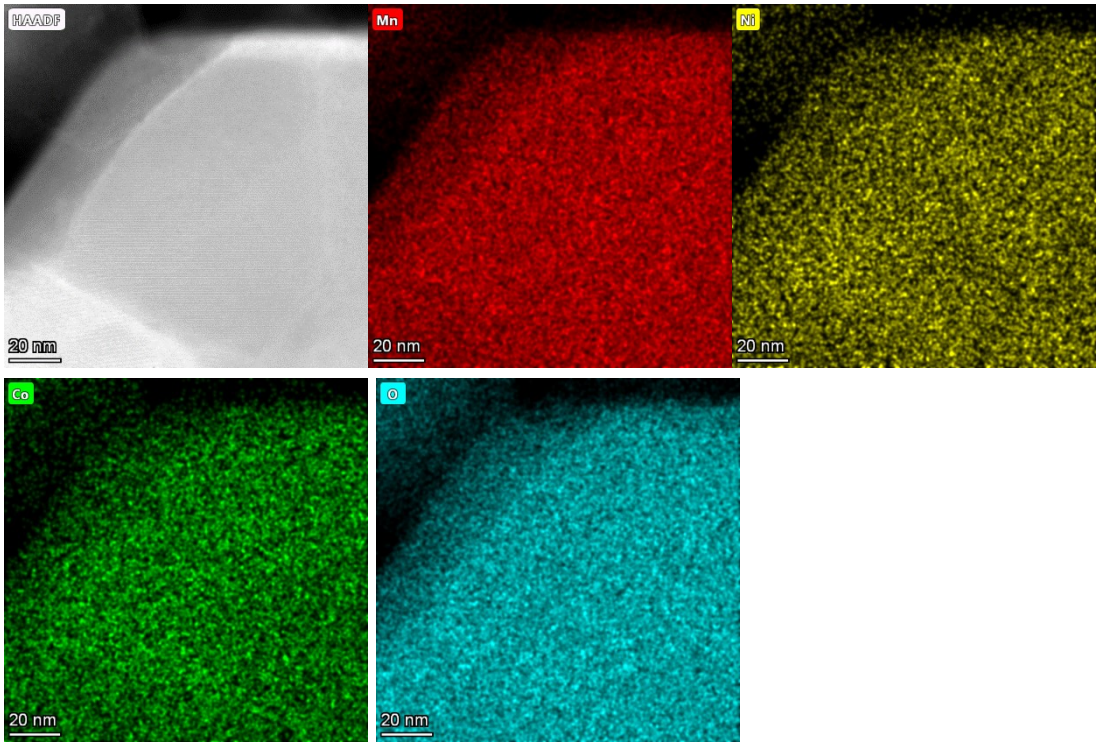

Figure S4. the EDS mapping of LMLO

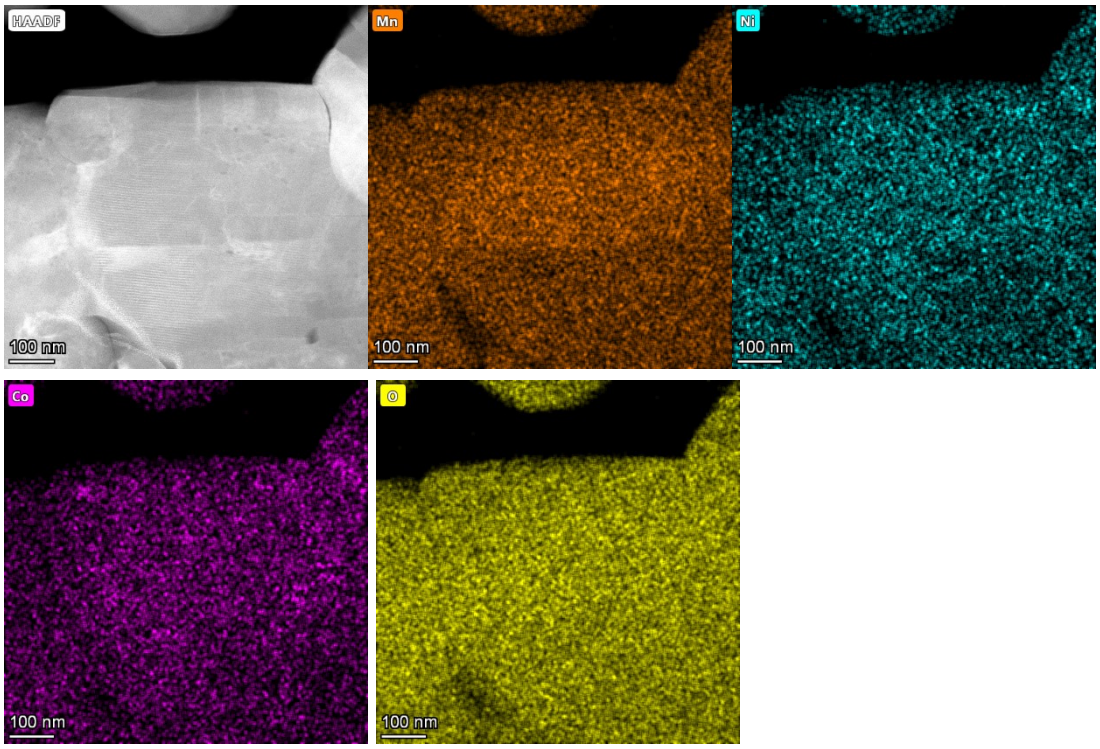

Figure S5. the EDS mapping of LMLO-Ov

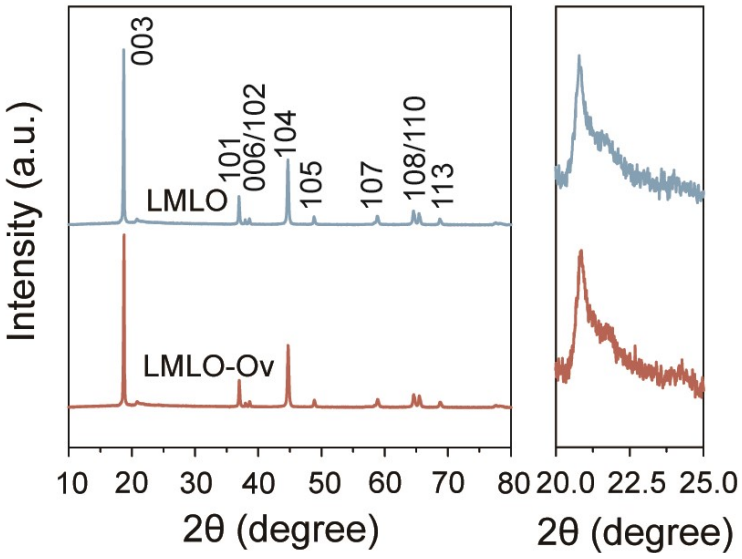

Figure S6. XRD of LMLO and LMLO-Ov

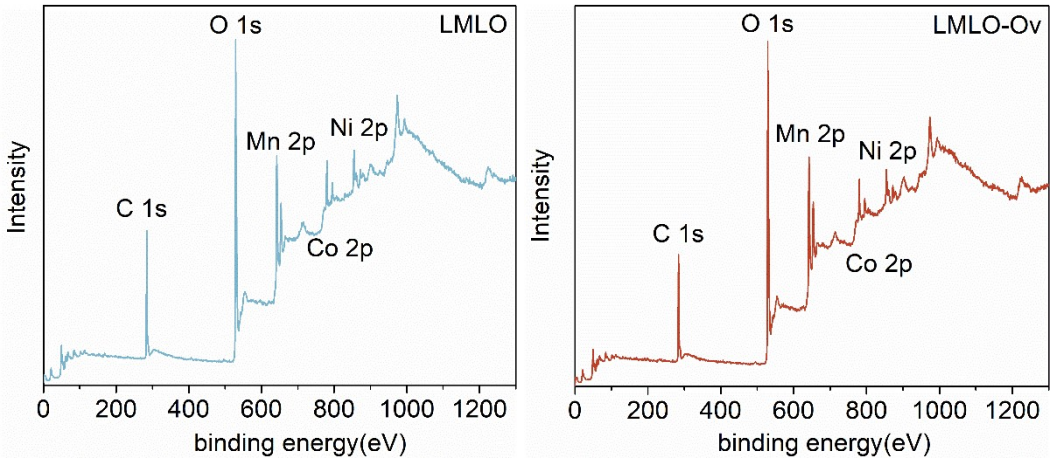

Figure S7. XPS survey spectra of LMLO and LMLO-Ov

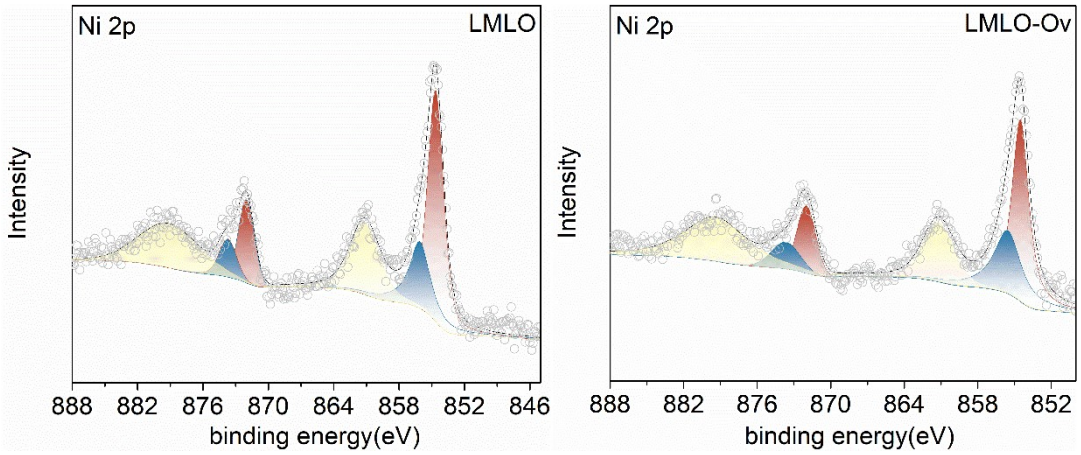

Figure S8. XPS Ni 2p spectra of LMLO and LMLO-Ov

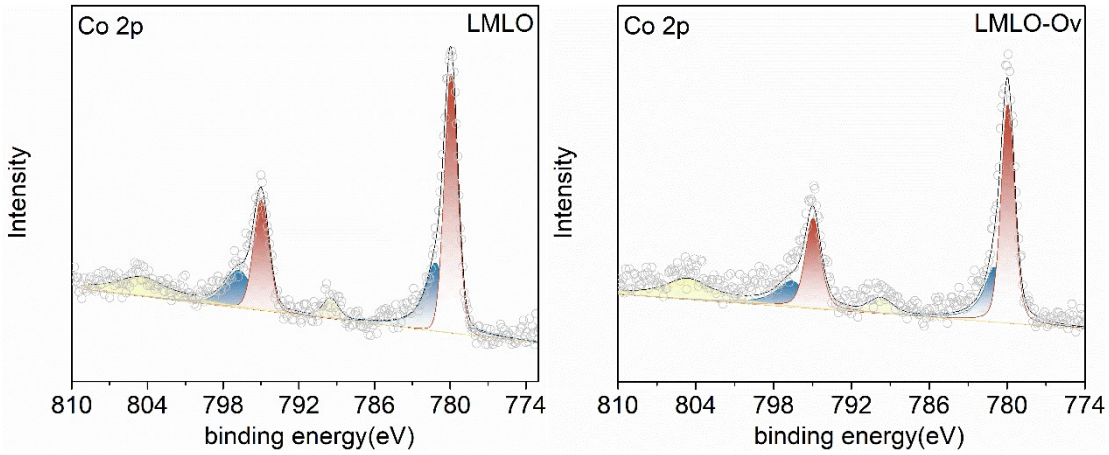

Figure S9. XPS Co 2p spectra of LMLO and LMLO-Ov

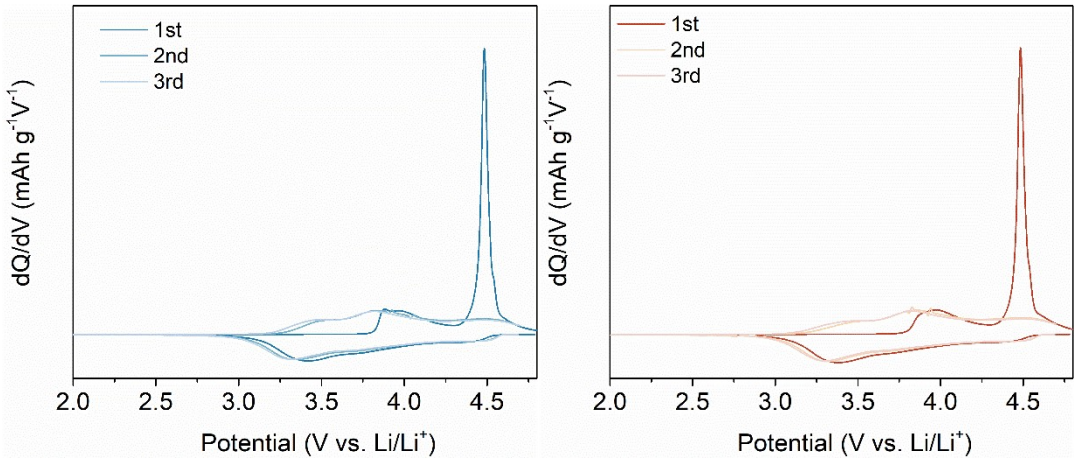

Figure S10. the dQ/dV curves of LMLO and LMLO-Ov

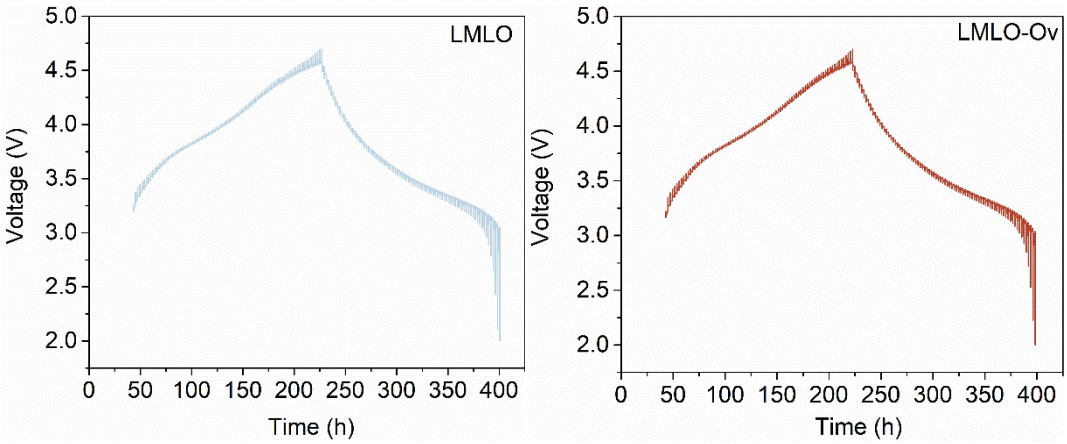

Figure S11. Titration time and voltage curve of LMLO and LMLO-Ov during the initial charging/discharging.

Table S1. Comparison of Methods for Introducing Spinel and Oxygen Vacancies on the Surface of Lithium-Rich Manganese Cathode Materials

References	Reaction temperature	Reaction time	reaction atmosphere	energy consumption
[1]	400℃	2h	NH_3	25.2MJ
[2]	500℃	~50h	Air	630MJ
[3]	400℃	3h	CO_2+NH_3	37.8MJ
[4]	500℃	3h	CO+CO_2	37.8MJ
[5]	350℃	6h	HCl+NH_3	75.6MJ
[6]	400℃	2h	NH_3+HF+BF_3	25.2MJ
[7]	200℃	10h	CO_2	126MJ
This work	1440K	8s	Ar	0.015MJ

We compared the current methodologies for introducing coating layers on the surface of Li-rich Mn-based layered oxides, focusing on reaction temperature, reaction time, reaction atmosphere, and energy consumption. Energy consumption is calculated using the formula Q = P * t, where P is power and t is time. The power is assumed to be approximately 3.5 kW, typical for laboratory furnaces. For the method we developed, energy consumption is calculated using $Q = I^2Rt$, where I is the current, R is the resistance of the heating system, and t is time. The pertinent results are presented in the table above. Comparative analysis reveals that the reaction time and energy consumption required for our developed method are markedly lower than those of current techniques, demonstrating exceptional efficiency and greater suitability for industrial production.

Table S2 XRD refinement results of LMLO

Space Group:R-3m Phase Ratio: 49.5%				
Lattice Parameters	a (Å)	b (Å)	c (Å)	V (Å^3)
	2.851	2.851	14.226	100.130
Space Group:C2/m Phase Ratio: 50.5%				
Lattice Parameters	a (Å)	b (Å)	c (Å)	V (Å^3)
	4.947	8.545	5.023	200.753
Agreement Factors				
Rwp 3.03% Rp 2.29%				

Table S3 XRD refinement results of LMLO-Ov

Space Group:R-3m Phase Ratio: 46.105%				
Lattice Parameters	a (Å)	b (Å)	c (Å)	V (Å^3)
	2.851	2.851	14.224	100.114
Space Group:C2/m Phase Ratio: 53.610%				
Lattice Parameters	a (Å)	b (Å)	c (Å)	V (Å^3)
	4.951	8.544	5.028	200.863
Space Group:Fd-3m Phase Ratio: 0.285%				
Lattice Parameters	a (Å)	b (Å)	c (Å)	V (Å^3)
	8.156	8.156	8.156	542.528
Agreement Factors				
Rwp 3.11% Rp 2.34%				

References

1. E. M. Erickson, H. Sclar, F. Schipper, J. Liu, R. Tian, C. Ghanty, L. Burstein, N. Leifer, J. Grinblat, M. Talianker, J.-Y. Shin, J. K. Lampert, B. Markovsky, A. I. Frenkel and D. Aurbach, *Adv. Energy Mater.*, 2017, **7**, 1700708.
2. K. Wang, J. Qiu, F. Hou, M. Yang, K. Nie, J. Wang, Y. Hou, W. Huang, W. Zhao, P. Zhang, J. Lin, J. Hu, F. Pan and M. Zhang, *Adv. Energy Mater.*, 2023, **13**, 2301216.
3. Y. Yang, Q. Zhu, J. Yang, H. Liu, Y. Ren, X. Sui, P. Wang, G. Sun and Z. Wang, *Adv. Funct. Mater.*, 2023, **33**, 2304979.
4. Z. Ye, B. Zhang, T. Chen, Z. Wu, D. Wang, W. Xiang, Y. Sun, Y. Liu, Y. Liu, J. Zhang, Y. Song and X. Guo, *Angew. Chem. Int. Ed.*, 2021, **60**, 23248-23255.
5. W. Yu, L. Zhao, Y. Wang, C. Yang, J. Wang, H. Huang, A. Wu, X. Dong and G. Cao, *J. Colloid Interface Sci.*, 2023, **648**, 820-833.
6. X. Gao, S. Li, H. Zhang, S. Zhang, S. Chang, H. Li, S. Li, Y. Lai and Z. Zhang, *Mater. Today Energy*, 2022, **30**, 101152.
7. B. Qiu, M. Zhang, L. Wu, J. Wang, Y. Xia, D. Qian, H. Liu, S. Hy, Y. Chen, K. An, Y. Zhu, Z. Liu and Y. S. Meng, *Nat. Commun.*, 2016, **7**, 12108.